



Title	Genetic consequences of habitat fragmentation in a perennial plant <i>Trillium camschatcense</i> are subjected to its slow-paced life history
Author(s)	Tsuzuki, Yoichi; Sato, Mitsuhiro P.; Matsuo, Ayumi; Suyama, Yoshihisa; Ohara, Masashi
Citation	Population Ecology, 64(1), 5-18 <a href="https://doi.org/10.1002/1438-390X.12093">https://doi.org/10.1002/1438-390X.12093</a>
Issue Date	2022-01
Doc URL	<a href="http://hdl.handle.net/2115/87602">http://hdl.handle.net/2115/87602</a>
Rights	This is the peer reviewed version of the following article: Yoichi Tsuzuki, Mitsuhiro P. Sato, Ayumi Matsuo, Yoshihisa Suyama, Masashi Ohara. Genetic consequences of habitat fragmentation in a perennial plant <i>Trillium camschatcense</i> are subjected to its slow-paced life history. Population Ecology, 2022; 64(1): 5-18, which has been published in final form at <a href="https://doi.org/10.1002/1438-390X.12093">https://doi.org/10.1002/1438-390X.12093</a> . This article may be used for non-commercial purposes in accordance with Wiley Terms and Conditions for Use of Self-Archived Versions.
Type	article (author version)
Additional Information	There are other files related to this item in HUSCAP. Check the above URL.
File Information	PopulationEcology_Tsuzuki_et_al_2021.pdf



[Instructions for use](#)

1 **Article Category:** Original Article

2

3 Genetic consequences of habitat fragmentation in a perennial plant *Trillium*

4 *camschatcense* are subjected to its slow-paced life history

5

6 Yoichi Tsuzuki<sup>1\*</sup>, Mitsuhiko P. Sato<sup>2</sup>, Ayumi Matsuo<sup>2</sup>, Yoshihisa Suyama<sup>2</sup>, Masashi

7 Ohara<sup>1</sup>

8

9 1. Graduate School of Environmental Science, Hokkaido University, N10W5, Sapporo,  
10 Hokkaido, 060-0810, Japan

11 2. Kawatabi Field Science Center, Graduate School of Agricultural Science, Tohoku  
12 University, 232-3 Yomogida, Naruko-onsen, Osaki, Miyagi, 989-6711, Japan

13 \* corresponding author: yoichi.tsuzuki.95@gmail.com

14

15 **Abstract**

16 Many wild populations are suffering from the loss of genetic diversity caused by habitat  
17 fragmentation, while the degree of diversity loss differs among species and populations  
18 based on their life history characteristics. *Trillium camschatcense*, an understory  
19 perennial plant, has undergone intensive habitat fragmentation in the Tokachi region,  
20 Hokkaido, Japan. Although demographic deteriorations, such as reduced seed  
21 production, were already reported, genetic consequences of fragmentation have not been  
22 studied with reference to its life history. Here, we examined how life history events  
23 (e.g., growth and reproduction) and the stochasticity therein influence genetic diversity  
24 in two (each large and small) fragmented *T. camschatcense* populations. Genetic  
25 diversity was evaluated using genome-wide 2,008 single nucleotide polymorphisms  
26 (SNPs). In the small population, genetic diversity of newly germinated seedlings was  
27 significantly lower than that of matured life history stages, and effective number of  
28 breeders ( $N_b$ ) was smaller than that of the large population. Simulations using a matrix  
29 population model showed that the diversity loss at seedlings is caused by genetic drift  
30 during reproduction, which was intensified by smaller  $N_b$ . Besides, simulations using  
31 randomly perturbed transition matrices suggested that stasis at juvenile stages, which is  
32 a common characteristics of *T. camschatcense*, maintains genetic diversity by buffering  
33 stochastic decrease, possibly contributing to population viability. While previous studies  
34 showed the importance to facilitate reproduction and recruitment for demographic  
35 recovery, this study highlighted the crucial roles of juvenile survival in terms of genetic  
36 diversity for the conservation of fragmented *T. camschatcense* populations in the  
37 Tokachi region.

38

39 **Keywords**

40 demographic genetic structure, demographic stochasticity, genetic drift, matrix

41 population model, stasis

## 42 **1 Introduction**

43 Anthropogenic land-use changes have been causing habitat loss and fragmentation  
44 worldwide, resulting in local extinction of many plant populations (Aguilar et al., 2018;  
45 Krauss et al., 2010). Small fragmented populations suffer from demographic and  
46 environmental stochasticity, both of which accelerate population shrinkage (Lande,  
47 1988). Besides, habitat fragmentation is predicted to decrease genetic diversity through  
48 bottleneck, genetic drift, restricted gene flow, and inbreeding (Aguilar, Quesada,  
49 Ashworth, Herrerias-Diego, & Lobo, 2008; Lowe, Boshier, Bacles, & Navarro, 2005;  
50 Young, Boyle, & Brown, 1996). Reduction in genetic diversity not only constrains the  
51 evolutionary potential (Bakker, van Rijswijk, Weissing, & Bijlsma, 2010; Ramsayer,  
52 Kaltz, & Hochberg, 2012), but could also suppress individual fitness and population  
53 growth (Reed & Frankham, 2003; Williams, 2001), thus threatening population  
54 viability. Hence, it is necessary to evaluate and mitigate the genetic impacts of habitat  
55 fragmentation on remnant populations.

56         Although many studies indicate that population shrinkage is a major driver of  
57 genetic diversity loss (Leimu, Mutikainen, Koricheva, & Fischer, 2006; Lowe et al.,  
58 2005), the susceptibility of genetic diversity to population decline differs among species  
59 and populations depending on their life history characteristics (Aguilar et al. 2008;  
60 González, Gómez-Silva, Ramírez, & Fontúrbel, 2019; Kramer, Ison, Ashley, & Howe,  
61 2008). Life history is a lifetime trajectory of individuals from birth to death, and  
62 because genetic information is stored in individuals, genetic dynamics is fundamentally  
63 subjected to life history (Li, Kurokawa, Giaimo, & Traulsen, 2016). In perennial plants,  
64 for example, slow growth and prolonged lifespan could allow old-aged individuals to  
65 persist for many years, resulting in slow generation turnover and delayed loss of genetic

66 diversity (Aparicio, Hampe, Fernández-Carrillo, & Albaladejo, 2012; Martins et al.,  
67 2015). It is important, therefore, to account for life history features to successfully  
68 assess genetic impacts of habitat fragmentation.

69         One way to take the entire life history into account is to comparatively evaluate  
70 genetic diversity among different age or stage classes. The resultant genetic structure is  
71 referred to as demographic genetic structure (Aldrich, Hamrick, Chavarriaga, &  
72 Kochert, 1998), and can reflect genetic consequences of all life history events, such as  
73 growth and reproduction. For example, comparison between reproductive adults and  
74 newborn progenies enables us to assess how much genetic drift during reproduction  
75 decreases genetic diversity (Aguilar et al. 2008). Moreover, demographic genetic  
76 structure could reveal potential genetic changes that accompany generation turnover  
77 from mature to juvenile individuals, providing an early-warning signal of diversity loss  
78 in fragmented populations (Aldrich et al., 1998; Ally & Ritland, 2006). However,  
79 demographic genetic structure is a static and momentary data because it is usually  
80 obtained at a single time point. Evaluating the long-term genetic changes requires  
81 additional knowledge on temporal dynamics. Integrating population dynamics models,  
82 which describe temporal changes in population size based on an individual survival and  
83 reproduction, with genetic data would be an effective solution.

84         *Trillium camschatcense* is an understory perennial plant which is widely  
85 distributed in northeast Asia including Japan, Russia, and Korean Peninsula. The center  
86 of its distributional range is Hokkaido, northern Japan. Although this species was once  
87 abundant in Hokkaido, its habitats have been destroyed due to agricultural and  
88 residential land development since the late 19th century (Ohara, Toimmatsu, Takada, &  
89 Kawano, 2006). One of the most striking habitat destructions took place in the Tokachi

90 region (Figure 1(a)). According to the records in the early time of land development  
91 (Hokkaido Government, 1897), this region had been almost completely forested, and  
92 understory plants including *T. camschatcense* were extensively distributed. However,  
93 intensive land development which started in the 1880s resulted in many small forest  
94 fragments within an agricultural matrix (Figure 1(b)). Previous studies have shown that  
95 the fragmentation restricts both seed production and the establishment of seedlings  
96 (Tomimatsu & Ohara, 2002; Tomimatsu & Ohara, 2004). Besides, a matrix population  
97 model, which was parameterized by individual survival rates and fecundity at every life  
98 history stage, was constructed based on six years of demographic monitoring in four  
99 fragmented populations (Tomimatsu & Ohara, 2010). Despite these achievements,  
100 genetic consequences of habitat fragmentation have not been well clarified in this  
101 system, although bottleneck effect was revealed by allozyme analysis on flowering  
102 individuals (Tomimatsu & Ohara, 2003).

103           Here, we combined empirically estimated demographic genetic structure with  
104 the previously constructed matrix population model and assessed how habitat  
105 fragmentation interacts with life history to influence genetic diversity and its long-term  
106 temporal dynamics of *T. camschatcense* in the Tokachi region.

107

108

## 109 **2 Materials and Methods**

### 110 **2.1 Study system**

111 *Trillium camschatcense* is a long-lived understory polycarpic plant. As with many other  
112 understory perennials, this species grows slowly with limited sunlight, taking a long  
113 period of years to become sexually mature. The prolonged life cycle can be categorized

114 into five distinct life history stages: seed (SE), seedling (SD), one-leaf (1L), three-leaves  
115 (3L), and flowering (FL) (Figure 2). Seeds germinate after two years of dormancy and  
116 grow as seedlings for the second year. From the third year on, they continue to grow as  
117 one-leaf and subsequently as three-leaves. It is not until they store enough assimilated  
118 resources that they become flowering. Flowering individuals are long-lived and remain  
119 reproductive for years, and sometimes retrogress to three-leaves due to resource  
120 exhaustion (Ohara & Kawano, 2005).

121 In May 2018, we selected 24 populations differing in habitat areas. We  
122 established one to three 5 m × 5 m quadrats in each population and recorded the number  
123 of flowering individuals within the quadrats. As a result, we found a significant positive  
124 effect of the habitat size on the density of FL (Figure 3). We selected two representative  
125 populations along the correlation: FUJ (Fuji town, Obihiro city), which is one of the  
126 largest populations in the region (density of FL = 328/25 m<sup>-2</sup>, habitat area = 5.87 ha),  
127 and SAK (Sakuragi town, Obihiro city), which is a small and severely fragmented  
128 population (density of FL = 104/25 m<sup>-2</sup>, habitat area = 0.71 ha).

129

## 130 **2.2 Sampling and SNP detection**

131 In May 2019, we established one 5 m × 5 m quadrat in each population and randomly  
132 collected leaves of 16 individuals per stage within each quadrat. We used random  
133 samples from the quadrat rather than from the entire population for two reasons. Firstly,  
134 considering that seeds of *T. camschatcense* were dispersed by ants up to only a few  
135 meters (Ohara & Higashi, 1987), the genetic composition could be highly spatially  
136 structured within a population. Therefore, the larger the sampling area is, the higher the  
137 estimated genetic diversity can be. To evaluate the role of life history independently



138 from that of sampling area, it is thus necessary to adopt a fixed spatial scale. Secondly,  
139 there is a need to adjust spatial scale of genetic data to that of the matrix population  
140 model parameterized by fine-scale demographic data (Tomimatsu & Ohara, 2010) for  
141 the later analysis. Because it was difficult to search and collect dormant seeds from soil,  
142 we omitted sampling from the seed stage (SE). Besides, considering that there was a  
143 large variation in plant size within 3L stage, we divided 3L into small (3L-1) and large  
144 (3L-2) stages based on leaf size (leaf length  $\times$  leaf width) with threshold of 150 cm<sup>2</sup>  
145 (approximately the midpoint of the leaf size range of 3L, see Supporting Information 1).  
146 As a result, 160 samples were collected in total (16 indiv./stage  $\times$  5 stages (SD, 1L, 3L-1,  
147 3L-2, FL)  $\times$  2 populations). The collected leaves were first stored in the refrigerator and  
148 then dried using silica gel. Genomic DNA was extracted from the dried leaves following  
149 the modified CTAB method (Murray & Thompson, 1980).

150 To quantify genetic diversity, we used multiplex ISSR genotyping by  
151 sequencing (MIG-seq; Suyama & Matsuki, 2015). MIG-seq is one of the reduced-  
152 representation DNA sequencing techniques and detects putatively neutral genome-wide  
153 SNPs adjacent to microsatellite regions. We followed the method modified from  
154 Suyama and Matsuki (2015) to prepare MIG-seq library. Sequencing was performed on  
155 an Illumina MiSeq Sequencer (Illumina, San Diego, CA, USA) using an MiSeq Reagent  
156 Kit v3 (150 cycle paired-end; Illumina). The sequence data is available at DDBJ with  
157 Accession number DRA009621.

158 Primer regions, adapter sequences, and low-quality reads were removed using  
159 Trimmomatic (Bolger, Lohse, & Usadel, 2014). The remaining reads were used for *de*  
160 *novo* assembly. SNPs were called using Stacks ver. 2.4 (Rochette, Rivera-Colón, &  
161 Catchen, 2019). Firstly, for each sample, sequenced reads were classified into groups

162 named “stack,” in which the number of nucleotide mismatch was two or less ( $M = 2$ ).  
163 The minimum number of reads required to form a stack is set to three ( $m = 3$ ).  
164 Ungrouped reads were aligned against the assembled stacks with a more permissive  
165 criterion: four nucleotide mismatches were allowed at maximum ( $N = 4$ ). Stacks from  
166 different samples were then aligned with one another to create a locus if the number of  
167 nucleotide mismatch was two or less ( $n = 2$ ). These parameter values are the default of  
168 Stacks *de novo* assembly. After these alignment procedures, SNPs which were  
169 successfully typed in at least 80% of all samples ( $r = 0.8$ ,  $p = 1$ ) were extracted with  
170 additional two criteria: minimum allele frequency must exceed 0.01 ( $\text{min-maf} = 0.01$ )  
171 and observed heterozygosity must be below or equal to 0.6 ( $\text{max-obs-het} = 0.6$ ). Among  
172 the extracted SNPs, we randomly selected one SNP per locus to avoid strong linkage  
173 ( $\text{write-random-snp}$ ). The resultant 2,008 SNPs were used for the following analyses.

174 To confirm the robustness of the results, we also called SNPs using various  $m$ ,  
175  $M$ ,  $N$ , and  $r$  ( $m = 3, 5, 8$ ;  $M = 1, 2, 3$ ;  $N = M + 2$ ;  $r = 0.7, 0.8, 0.9$ ). Different  $m$ ,  $M$ , and  
176  $N$  were used with  $r$  being kept at 0.8, while different  $r$  values were used under the  
177 default  $m$ ,  $M$ , and  $N$  (i.e.,  $m = 3$ ,  $M = 2$ ,  $N = 4$ ). Besides, to evaluate the influence of  
178 missing data, we excluded samples in which more than 30 % of SNPs were missing  
179 when  $m$ ,  $M$ ,  $N$ , and  $r$  were 3, 2, 4, and 0.8, respectively. Because these various settings  
180 yielded qualitatively similar results, we only present the results of the following  
181 parameter settings:  $m = 3$ ,  $M = 2$ ,  $N = 4$ ,  $r = 0.8$ . The results under the other parameter  
182 values were available in Supporting Information 2.

183

### 184 **2.3 Demographic genetic structure**

185 Allelic richness ( $A_R$ ), effective number of alleles ( $A_E$ ), observed heterozygosity ( $H_O$ ),

186 expected heterozygosity ( $H_E$ ), gene diversity ( $H_S$ ), and standardized multilocus  
187 heterozygosity (sMLH), were calculated for each life history stage. Allelic richness is  
188 the number of alleles adjusted by rarefaction. Effective number of alleles is the inverse  
189 of the sum of squared allele frequencies and reflects not only the number but also the  
190 evenness of alleles in a population. While expected and observed heterozygosity are  
191 conventionally used to quantify intrapopulation diversity, gene diversity is an unbiased  
192 estimator of expected heterozygosity for small sample size (Nei & Chesser, 1983).  
193 Standardized multilocus heterozygosity is the proportion of heterozygous loci in an  
194 individual divided by the average observed heterozygosity in the population over the  
195 subset of loci successfully typed in the focal individual, and is thus measured on an  
196 identical scale for all individuals (Coltman, Pilkington, Smith, & Pemberton, 1999).  
197 Inbreeding coefficient ( $F_{IS}$ ), which represents the level of inbreeding and is expected to  
198 increase with time in isolated populations, was also estimated. All metrics except  $H_E$   
199 and sMLH were calculated with the modified function of “allelic.richness” and  
200 “basic.stats” in R package “hierfstat” (Goudet, 2005), and the R code is provided in  
201 Supporting Information 3.  $H_E$  and sMLH were calculated using the function “Hs” and  
202 “sMLH” in R package “adegenet” and “inbreedR”, respectively (Jombart, 2008; Stoffel  
203 et al., 2016).

204         Permutation test was used to evaluate whether genetic diversity ( $A_R$ ,  $A_E$ ,  $H_O$ ,  
205  $H_E$ ,  $H_S$ , and mean sMLH) became lower and inbreeding coefficients ( $F_{IS}$ ) became  
206 higher in more juvenile stages. For all pairs of two stages, we randomly shuffled the  
207 assignment of stages to individuals without replacement and calculated the seven  
208 metrics. We subtracted the diversity estimates ( $A_R$ ,  $A_E$ ,  $H_O$ ,  $H_E$ ,  $H_S$ , and mean sMLH)  
209 of more juvenile stage from those of more matured stage, while subtracting  $F_{IS}$  of more

210 matured stage from that of more juvenile stage. The subtracted values were used as test  
211 statistics, and their null distributions were generated by repeating these procedures for  
212 999 times. The one-sided  $p$ -value was obtained as the frequency of 999 simulated and  
213 one observed value greater than or equal to the observed value.  $P$ -values were adjusted  
214 by sequential Bonferroni method for multiple comparison. The R code used for  
215 permutation test is provided in Supporting Information 4.

216

#### 217 **2.4 Effective number of breeders**

218 Effective number of breeders ( $N_b$ ) is the counterpart of effective population size ( $N_e$ )  
219 per single reproductive season, not per generation (Waples & Teel, 1990).  $N_b$  represents  
220 the idealized number of reproductive individuals showing the same rate of genetic  
221 diversity loss from adults to offspring as the observed data. “Idealized” means that  
222 adults randomly mate and produce the same number of offspring as themselves.  $N_b$   
223 reflects any factors involved in reproduction, such as the number of mating individuals  
224 and the per capita fecundity. Hence, the reduction in genetic diversity from flowering  
225 (FL) to seedlings (SD) during reproduction could be well evaluated by  $N_b$ .

226 In estimating  $N_b$ , we followed the method of Hui and Burt (2015), which  
227 estimates  $N_e$  from allele frequency data of different generations using maximum  
228 likelihood method. Here, we assumed FL and SD as two consecutive generations. This  
229 assumption is realistic, because SD is a two-year-old cohort whose parents are likely to  
230 remain in FL considering the rarity of individual turnover in the flowering stage in this  
231 species (Ohara & Kawano, 2005). We used these two “generations” to estimate  $N_b$  using  
232 the function “NB. estimator” in R package “NB” (Hui & Burt, 2015).

233

234 **2.5 Model structure**

235 We used a matrix population model to simulate the temporal dynamics of genetic  
 236 diversity for FUJ and SAK populations. Matrix population models are usually used to  
 237 predict discrete-time population dynamics of age- or stage-structured populations and  
 238 consist of demographic rates, which are survival rates and fecundity of each age/stage  
 239 class (Caswell, 2001). In *T. camschatcense*, which has five life history stages (SE, SD,  
 240 1L, 3L, and FL), annual population dynamics can be modeled as follows:

$$241 \begin{pmatrix} n_{SE,t+1} \\ n_{SD,t+1} \\ n_{1L,t+1} \\ n_{3L,t+1} \\ n_{FL,t+1} \end{pmatrix} = \begin{pmatrix} 0 & 0 & 0 & 0 & f \\ g_0 & 0 & 0 & 0 & 0 \\ 0 & g_1 & s_2 & 0 & 0 \\ 0 & 0 & g_2 & s_3 & r_4 \\ 0 & 0 & 0 & g_3 & s_4 \end{pmatrix} \begin{pmatrix} n_{SE,t} \\ n_{SD,t} \\ n_{1L,t} \\ n_{3L,t} \\ n_{FL,t} \end{pmatrix} \quad (1)$$

242  $n_{i,t}$  denotes the number of individuals in stage  $i$  in year  $t$ . Elements in the matrix include  
 243 the probabilities of germination ( $g_0$ ), growth ( $g_1, g_2, g_3$ ), stasis (remaining in the same  
 244 stage;  $s_2, s_3, s_4$ ), retrogression (going backward to previous stage;  $r_4$ ), and fecundity ( $f$ )  
 245 per year (Figure 4). Because it is unfeasible to track the survival/death of dormant seeds  
 246 in field, fecundity is usually estimated as a product with the germination rate in the next  
 247 year, as in Tomimatsu and Ohara (2010). To separate  $f$  and  $g_0$ , we assumed that the  $g_0$   
 248 was either 0.2, 0.4, 0.6, 0.8, or 1, and carried out the following analyses for each case.

249 We applied the matrix population model to predict temporal changes in allele  
 250 frequencies. We assumed a biallelic neutral locus with alleles  $A$  and  $a$ . Since *T.*  
 251 *camschatcense* is a diploid species, there can be three genotypes:  $AA$ ,  $Aa$ , and  $aa$ . The  
 252 transition probabilities (i.e., growth, stasis, and retrogression probabilities) and the  
 253 fecundity were set to be equal among all genotypes. The number of individuals per  
 254 genotype per stage can be predicted by extending the model as follows.

$$\begin{matrix} 255 \\ 256 \end{matrix}
\begin{pmatrix} N_{SE,t+1} \\ N_{SD,t+1} \\ N_{1L,t+1} \\ N_{3L,t+1} \\ N_{FL,t+1} \end{pmatrix} = \begin{pmatrix} \mathbf{O} & \mathbf{O} & \mathbf{O} & \mathbf{O} & \mathbf{F} \\ \mathbf{G}_0 & \mathbf{O} & \mathbf{O} & \mathbf{O} & \mathbf{O} \\ \mathbf{O} & \mathbf{G}_1 & \mathbf{S}_2 & \mathbf{O} & \mathbf{O} \\ \mathbf{O} & \mathbf{O} & \mathbf{G}_2 & \mathbf{S}_3 & \mathbf{R}_4 \\ \mathbf{O} & \mathbf{O} & \mathbf{O} & \mathbf{G}_3 & \mathbf{S}_4 \end{pmatrix} \begin{pmatrix} N_{SE,t} \\ N_{SD,t} \\ N_{1L,t} \\ N_{3L,t} \\ N_{FL,t} \end{pmatrix} \quad (2)$$

256  $N_{i,t}$  denotes the vector of the number of individuals in stage  $i$  in year  $t$

$$\begin{matrix} 257 \end{matrix}
\mathbf{N}_{i,t} = \begin{pmatrix} n_{i,AA,t} \\ n_{i,Aa,t} \\ n_{i,aa,t} \end{pmatrix} \quad (3)$$

258 where  $n_{i,j,t}$  denotes the number of individuals of genotype  $j$  in stage  $i$  in year  $t$ . The  
259 summation of  $N_{i,t}$  is equal to  $n_{i,t}$ . The first matrix of the right side of Equation (2)  
260 consists of  $3 \times 3$  submatrices which are shown in capital letters.  $\mathbf{O}$  is a zero matrix,  
261 while the other submatrices except  $\mathbf{F}$  are diagonal matrices whose diagonal elements are  
262 the small letters of themselves. For example, the submatrix  $\mathbf{G}_1$  is given by

$$\begin{matrix} 263 \end{matrix}
\mathbf{G}_1 = \begin{pmatrix} g_1 & 0 & 0 \\ 0 & g_1 & 0 \\ 0 & 0 & g_1 \end{pmatrix} \quad (4)$$

264 and the other submatrices except  $\mathbf{F}$  are similarly set. The use of diagonal submatrices  
265 holds because genotype of an individual never changes over the course of life history  
266 except reproduction, where gametes are shuffled. In deriving  $\mathbf{F}$ , we first defined  $p_{A,t}$  and  
267  $p_{a,t}$  as allele frequencies of  $A$  and  $a$  in FL in year  $t$ . Under complete random mating, a  
268 given gamete will form a zygote with  $A$  and  $a$  with the probability of  $p_{A,t}$  and  $p_{a,t}$ ,  
269 respectively. Considering that flowering individuals of  $AA$  produce only gametes of  $A$ ,  
270 their seeds can be split into  $AA$ ,  $Aa$ , and  $aa$  at the ratio of  $p_{A,t}$ ,  $p_{a,t}$ , and zero. Similarly,  
271 the proportions of  $AA$ ,  $Aa$ , and  $aa$  among the seeds of  $aa$  individuals are zero,  $p_{A,t}$ , and  
272  $p_{a,t}$ , respectively. In the case of  $Aa$  individuals which produce gametes of  $A$  and  $a$  in  
273 half, the genotypic composition of their seeds is the mean of that of  $AA$  and  $aa$   
274 flowering individuals:  $p_{A,t}/2$ ,  $1/2$  and  $p_{a,t}/2$  for  $AA$ ,  $Aa$ , and  $aa$ , respectively. Therefore,

275  $F$  satisfies the following equations.

$$276 \quad \mathbf{N}_{SE,t+1} = \mathbf{F} \mathbf{N}_{FL,t} = \begin{pmatrix} fp_{A,t} & fp_{A,t}/2 & 0 \\ fp_{a,t} & f/2 & fp_{A,t} \\ 0 & fp_{a,t}/2 & fp_{a,t} \end{pmatrix} \begin{pmatrix} n_{FL,AA,t} \\ n_{FL,Aa,t} \\ n_{FL,aa,t} \end{pmatrix} \quad (5)$$

277 The first to third column of  $F$  represent the composition of seeds produced by a  
278 flowering individual of  $AA$ ,  $Aa$ , and  $aa$ , respectively.

279 Since populations exponentially grow and become unrealistically large/small  
280 under the model analyses, the number of individuals in each stage was scaled at each  
281 timestep to remain constant. This assumption holds asymptotically in density-dependent  
282 structured population dynamics, as in Ellner (1996). We carried out simulations at a  
283 spatial scale of 25 m<sup>2</sup> by fixing  $n_{FL,t}$  to the density of flowering individuals per 25 m<sup>2</sup>  
284 surveyed in 2018 for each population, while the number of individuals of the other  
285 stages were set to be proportional to the stable stage structure, which is the leading right  
286 eigenvector of the transition matrix. We multiplied the fixed number and the ratio of  
287 three genotypes (i.e.,  $AA$ ,  $Aa$ ,  $aa$ ) calculated at each time step to yield the number of  
288 individuals per stage per genotype, allowing changes in genetic composition while  
289 keeping population size and stage structure constant.

290 We incorporated two stochastic processes, genetic drift and demographic  
291 stochasticity, into the model. Genetic drift is the probabilistic fluctuations in offspring  
292 allele frequency due to chance effect in random mating. Demographic stochasticity is  
293 the random deviation from expected population dynamics due to the probabilistic nature  
294 of individual survival and reproduction: whether to grow, stay, regress, or die is  
295 determined probabilistically and independently among individuals. To compare the  
296 genetic consequences between the two stochasticity, we carried out simulations under  
297 four scenarios: (1) no stochasticity, (2) only genetic drift, (3) only demographic

298 stochasticity, and (4) both genetic drift and demographic stochasticity.

299 The degree of genetic drift per year depends on effective number of breeders  
 300 ( $N_b$ ), and the allele frequencies of newborn seeds must be comparable with those of  $N_b$   
 301 seeds produced by a random mating of flowering individuals. Thus, we did multinomial  
 302 sampling  $N_b$  times based on the expected genotype frequencies of seeds in the next year  
 303 ( $AA: p_{A,t}^2; Aa: 2p_{A,t}p_{a,t}; aa: p_{a,t}^2$ ) to obtain perturbed frequencies of seeds under genetic  
 304 drift ( $\tilde{p}_{SE,AA,t+1}, \tilde{p}_{SE,Aa,t+1}, \tilde{p}_{SE,aa,t+1}$ ). We used  $N_b$  estimated from the empirical  
 305 genetic data for each population.  $N_{SE,t+1}$  can be calculated by the product of total  
 306 number of seeds (i.e.,  $n_{SE,t+1}$ , or  $f n_{FL,t}$ , in Equation (1)) and the perturbed genotype  
 307 frequencies.

$$308 \quad N_{SE,t+1} = f n_{FL,t} \times \begin{pmatrix} \tilde{p}_{SE,AA,t+1} \\ \tilde{p}_{SE,Aa,t+1} \\ \tilde{p}_{SE,aa,t+1} \end{pmatrix} \quad (6)$$

309 On the other hand, the degree of demographic stochasticity corresponds to the  
 310 actual number of individuals, not  $N_b$ , and the smaller the number is, the more likely  
 311 actual transition probability deviates from expectation. We used multinomial sampling  
 312 in transition processes (Figure 4).

$$313 \quad Multi(n_{i,j,t}; t_{SE,i}, t_{SD,i}, t_{1L,i}, t_{3L,i}, t_{FL,i}, d_i)$$

314  $t_{SE,i}, \dots, t_{FL,i}$  are the transition probabilities from stage  $i$  to the respective stages.  $d_i$  is the  
 315 mortality rate of stage  $i$ . Multinomial sampling from the above probability distribution  
 316 yields how individuals of genotype  $j$  in stage  $i$  in year  $t$  are split into all possible states  
 317 in the next year. As for reproduction, the number of seeds was taken from Poisson  
 318 distribution with mean equal to the value in the case without demographic stochasticity.  
 319 Mean of the distribution under scenario (3) and (4) can be calculated from Equation (5)



320 and (6), respectively. For example,  $n_{SE,AA,t+1}$  follows the Poisson distribution bellow.

$$321 \quad n_{SE,AA,t+1} \sim \begin{cases} Pois(fp_{A,t}n_{FL,AA,t} + fp_{A,t}n_{FL,Aa,t}/2) & \text{scenario 3} \\ Pois(f n_{FL,t} \tilde{p}_{SE,AA,t+1}) & \text{scenario 4} \end{cases}$$

322 The resultant number of individuals was then scaled to remain the same as the previous  
 323 year. To make multinomial sampling applicable, the scaled number was always rounded  
 324 off and adjusted to integer value.

325 All simulations were performed on R, and the code is provided in Supporting  
 326 Information 5.

327

## 328 **2.6 Simulation of the temporal genetic dynamics**

329 Tomimatsu and Ohara (2010) estimated annual transition probabilities and a two-year  
 330 fecundity (annual fecundity  $\times$  germination rate) in four fragmented *T. camschatcense*  
 331 populations in our study region from 2000 to 2006. We used the mean over the years  
 332 and the populations to construct a transition matrix.

$$333 \quad \begin{pmatrix} 0 & 0 & 0 & 0 & 6.197/g_0 \\ g_0 & 0 & 0 & 0 & 0 \\ 0 & 0.477 & 0.659 & 0 & 0 \\ 0 & 0 & 0 & 0.819 & 0.082 \\ 0 & 0 & 0 & 0.130 & 0.893 \end{pmatrix} \quad (7)$$

334 The numerator of the top-right element (6.197) is the estimated two-year fecundity,  
 335 which is divided by germination rate  $g_0$  to obtain annual fecundity. The initial ratio of  
 336 the three genotypes (*AA*, *Aa*, *aa*) was set to 1:2:1 for each stage. We then simulated 200  
 337 years of temporal dynamics of expected heterozygosity for 100 times under the four  
 338 scenarios as explained earlier. Average expected heterozygosity for each stage and year  
 339 were calculated.

340

## 341 **2.7 Dependence of genetic diversity on demographic rates**

342 To estimate the dependence of genetic diversity on each life history event, we evaluated  
343 the loss of genetic diversity in situations where demographic rates (i.e., transition  
344 probabilities and fecundity, or the none-zero matrix elements in Equation (7)) were  
345 randomly perturbed. We used uniform random numbers that deviate from 0 by up to 0.1  
346 for parameter perturbation, partly following the method of Takada and Kawai (2020).  
347 The detailed procedures can be available in Supporting Information 6. 500 random  
348 transition matrices were generated and were applied to FUJ and SAK populations as  
349 previously conducted with the original transition matrix. 200 years of temporal genetic  
350 changes were computed 100 times. Average expected heterozygosity ( $H_E$ ) over the 100  
351 iterations was calculated for each stage and year. For the total of 501 simulations (500  
352 random transition matrices and the original transition matrix), redundancy analysis  
353 (RDA) was used to examine the relationships between  $H_E$  of the five life history stages  
354 in the 200th year and demographic rates. The five  $H_E$  were ordinated with demographic  
355 rates as constraints, and the statistical significance of the overall ordination, subsequent  
356 RDA axes, and constraint variables were tested with 999 permutations (Borcard, Gillet,  
357 & Legendre, 2011). All analyses regarding RDA were carried out using an R package  
358 “vegan” (Oksanen et al., 2019).

359

360

### 361 **3. Results**

#### 362 **3.1 Demographic genetic structure**

363 Genetic diversity and inbreeding coefficient were estimated per stage per population  
364 (Figure 5). In FUJ (large) population, although all six diversity proxies gradually  
365 increased from seedlings (SD) to flowering (FL), there were no significant differences

366 among the five stages. On the other hand, in SAK (small) population, genetic diversity  
367 of SD was significantly lower than that of FL and 3L-2 for all six diversity indices  
368 (Figure 5(a)–(f)). Inbreeding coefficient was not significantly different among stages in  
369 both populations, yet it steadily decreased from SD to FL in SAK population (Figure  
370 5(g)).

371

### 372 **3.2 Effective number of breeders**

373 Effective number of breeders ( $N_b$ ) and its 95 percent confidence interval (C.I.) were  
374 estimated (FUJ:  $N_b = 25.8$ , C.I. = 18.9–39.1; SAK:  $N_b = 18.0$ , C.I. = 14.0–24.5).  $N_b$  of  
375 SAK population was lower than that of FUJ population. The confidence interval  
376 overlapped each other, indicating that the difference between the two populations was  
377 slight.

378

### 379 **3.3 Demographic genetic structure under different stochasticity situations**

380 Simulation analysis revealed 200 years of temporal dynamics of expected  
381 heterozygosity ( $H_E$ ) in both populations (Figure 6). Because the results are qualitatively  
382 similar among different  $g_0$ , we here present only the results of  $g_0 = 1$  (see Supporting  
383 Information 7 for the other  $g_0$ ). Without stochasticity, there were no differences in  $H_E$   
384 among the five stages with no temporal decline at all (Figure 6(a)). However,  $H_E$   
385 steadily decreased over the course of time if either or both stochasticity was present  
386 (Figure 6(b)–(d)).  $H_E$  of seedlings completely tracked that of seeds with one-year delay,  
387 reflecting the double dormancy of this species. The slope of temporal decrease was  
388 much steeper in SAK population than in FUJ population. Under the presence of genetic  
389 drift,  $H_E$  became lower along the maturity gradient (from matured to juvenile stages),

390 and  $H_E$  of seeds and seedlings was kept lower than that of the other three stages, which  
391 was more obvious in SAK population (Figure 6(b)(d)). When only demographic  
392 stochasticity was incorporated, no apparent inter-stage differences were found (Figure  
393 6(c)).

394

### 395 **3.4 Dependence of genetic diversity on demographic rates**

396 Associations between  $H_E$  of the five life history stages and demographic rates were  
397 visualized in RDA correlation triplots (Figure 7). Because we got similar results under  
398 different  $g_0$ , only the results of  $g_0 = 1$  were presented (see Supporting Information 8 for  
399 the other  $g_0$ ). RDA was not performed for scenario 1 because  $H_E$  always remained the  
400 same as the initial condition, hardly affected by demographic rates. In the other three  
401 scenarios, RDA axis 1 had prominent explanatory power (approximately 50–80 % of the  
402 total variance, Figure 7). In RDA triplots, the angles between  $H_E$  and demographic rates  
403 reflect their correlations, while signs of the axes are arbitrary (Borcard et al., 2011).  
404 Therefore, demographic rates that were in the same direction with the five  $H_E$  regarding  
405 RDA axis 1 likely significantly contributed to high  $H_E$ . As for scenario 2,  $s_2$  and  $s_3$   
406 (stasis of 1L and 3L) had relatively strong positive correlations with  $H_E$ , while  $g_2$  and  
407  $g_3$  (growth of 1L and 3L) had negative correlations (Figure 7(a)). In other words,  
408 populations with high stasis probabilities at juvenile stages maintained genetic diversity  
409 under genetic drift. In scenario 3,  $H_E$  were positively correlated with  $s_3$  (Figure 7(b)),  
410 indicating that genetic diversity was maintained when  $s_3$  was high under demographic  
411 stochasticity. In scenario 4,  $s_2$ , and  $s_3$  strongly boosted  $H_E$  under both stochasticity  
412 (Figure 7(c)).

413

414

## 415 **4 Discussion**

### 416 **4.1 Loss of genetic diversity in fragmented populations**

417 We revealed that genetic diversity of seedlings (SD) was significantly lower than that of  
418 flowering (FL) and three-leaves (3L-2) individuals in the small SAK population (Figure  
419 5(a)–(f)), and that  $N_b$  was slightly smaller in SAK than in FUJ population. Simulation  
420 results indicate that genetic drift causes the apparently lower expected heterozygosity of  
421 SE and SD compared to the other mature stages, especially in SAK population (Figure  
422 6(b)). Therefore, the low diversity of SD observed in SAK population could be  
423 attributed to genetic drift at reproduction: small  $N_b$  caused a greater sampling bias in the  
424 genetic composition of seeds and seedlings. These results agree with previous studies  
425 showing that smaller populations suffer from genetic drift more strongly than larger  
426 ones (Crow & Morton, 1955; Lowe et al., 2005; Toczydlowski & Waller, 2019).

427 Besides, the apparent, although not significant, increase in inbreeding  
428 coefficient of SD in SAK population (Figure 5(g)) suggests that strong genetic drift in  
429 SAK population might be accompanied by the increased level of inbreeding. Inbreeding  
430 causes greater decrease in observed than in expected heterozygosity and would alter  
431 genotypic composition. This might be partly responsible for the statistical significance  
432 only detected in SAK population despite the seemingly identical decrease in some  
433 indices (e.g., allelic richness) in both populations, because permutation of individuals  
434 can readily detect differences in genotypic composition which allele-based indices such  
435 as allelic richness are less sensitive to.

436 In contrast to genetic drift, demographic stochasticity did not induce consistent  
437 differences in genetic diversity among the five stages (Figure 6(c)). This could be

438 because that demographic stochasticity occurs at all stages and results in parallel  
439 decrease, while genetic drift acts at only reproduction and leads to imbalanced decline  
440 in SE and SD.

441           It should be noted that genetic diversity of SAK (small) population was almost  
442 at the same level as, or sometimes higher than, that of FUJ (large) population (Figure  
443 5(a)–(f)), which might seem inconsistent with the simulation results showing that  
444 genetic diversity decreases faster in SAK than in FUJ population and the previously  
445 reported bottleneck effect (Tomimatsu & Ohara, 2003). Besides, inbreeding coefficient  
446 was seemingly lower in SAK than in FUJ population (Figure 5(g)). It might be that  
447 SAK had been much larger and had higher diversity than FUJ before fragmentation.  
448 Large population could attract many pollinators (Tomimatsu & Ohara, 2002), and  
449 resultant extensive pollination, together with self-incompatibility of this species in the  
450 study region (Ohara, Takeda, Ohno, & Shimamoto, 1996), should have had lowered  $F_{IS}$   
451 in SAK population. Our results might have reflected these pre-fragmentation legacies  
452 due to the few generations passed after fragmentation (Tomimatsu & Ohara, 2006). The  
453 time elapsed since fragmentation itself might be shorter in SAK than in FUJ  
454 populations. Moreover, our sampling strategy did not aim at inter-population  
455 comparison: we sampled individuals from a fine 5 m × 5 m quadrat, not from the whole  
456 population, which can hardly detect bottleneck effect. Our focus is on the genetic  
457 differences among stages within a population, which can be evaluated separately from  
458 the differences among populations. The interpretation of the data is thus concrete  
459 despite the potential historical factors listed above.

460

#### 461 **4.2 Roles of life history events in maintaining genetic diversity**

462 High degree of stasis at 1L and 3L contributed to high genetic diversity under genetic  
463 drift in both populations (Figure 7(a)). As has been discussed above, genetic drift  
464 randomly perturbs genetic composition of SE and consequently SD year by year. Stasis  
465 enables individuals older in age to remain in juvenile stages and to coexist with younger  
466 ones, thereby mixing differently aged cohorts. Overlap of cohorts could offset annual  
467 randomness caused by genetic drift and thus maintain as the same level of genetic  
468 diversity in juveniles as in flowerings. This mechanism may be consistent with the  
469 storage effect, which was previously suggested by studies showing that generation  
470 overlap maintain genetic diversity under fluctuating selection pressures (Ellner, 1996;  
471 Ellner & Hairston, 1994). Our results also agree with the preceding finding that long  
472 lifespan could slow down generation turnover and thus delay diversity loss (Aparicio et  
473 al., 2012; Martins et al., 2015), because high stasis probabilities would extend lifespan.

474 Demographic stochasticity, the magnitude of which depends on the number of  
475 individuals (Lande, 1988), was mitigated by the increase in  $s_3$  (Figure 7(b)). Since  $s_3$   
476 could promote accumulation of individuals and thus reduce demographic stochasticity  
477 at 3L, the results indicate that buffering demographic stochasticity at 3L is crucial for  
478 maintaining genetic diversity of the whole population. In polycarpic perennial forest  
479 herbs, survival of established individuals, rather than annual reproduction, usually plays  
480 a predominant role in population dynamics (Silvertown, Franco, Pisanty, & Mandoza,  
481 1993). Because 3L constitutes large part of the survival process, its predominant  
482 contributions to the overall genetic dynamics might have been highlighted.

483 In the most realistic scenario where both genetic drift and demographic  
484 stochasticity occur (scenario 4), stasis at 1L and 3L maintained high genetic diversity.  
485 The high degree of stasis at juvenile stages is a common characteristic of  $T$ .

486 *camschatcense* (Ohara & Kawano, 2005), implying that the two examined populations  
487 might maintain genetic diversity and population viability unless its life history is not  
488 severely altered. In general, habitat fragmentation adversely affects survival and growth  
489 of plant seedlings (Aguilar et al., 2019). It would be necessary to examine if  
490 fragmentation also alters survival and growth of juveniles to evaluate the risk of genetic  
491 diversity loss.

492

493

## 494 **5. Conclusion**

495 The present study examined how life history events and the stochasticity therein interact  
496 with habitat fragmentation and influence genetic diversity of the two fragmented *T.*  
497 *camschatcense* populations in the Tokachi region. As a result, it was shown that genetic  
498 drift during reproduction causes significant diversity loss at seedlings especially in the  
499 small SAK population, and that stasis at 1L and 3L stages could buffer the stochasticity  
500 and maintain local genetic diversity in both populations. It should be noted that the  
501 comparison of two populations might be insufficient to draw general conclusions.  
502 However, considering that the two studied populations were representative in terms of  
503 FL density and habitat area (Figure 3), our discussion might be applicable to at least the  
504 other populations in the same region. While the need to facilitate reproduction and  
505 recruitment had been already highlighted from a demographic point of view (Ohara et  
506 al., 2006; Tomimatsu & Ohara, 2002; Tomimatsu & Ohara, 2004), this study, for the  
507 first time, revealed the importance of the survival of established individuals in terms of  
508 genetic diversity. Taken together, it is suggested that the whole life history processes  
509 should be considered for the conservation in fragmented *T. camschatcense* populations



510 in the Tokachi region.

511

512

### 513 **Acknowledgements**

514 We thank landowners, Obihiro City government, and Hiroo Town government for  
515 kindly allow our fieldwork. We are also grateful to T. Takada for his advice on our  
516 simulation analysis. This study was supported by Sasakawa Scientific Research Grant  
517 from the Japan Science Society (2019-5027) and Grants-in-Aid for Scientific Research  
518 from the Japan Society for the Promotion of Science (19H03294 and 20K06821).

519

520

### 521 **References**

522 Aguilar, R., Quesada, M., Ashworth, L., Herrerias-Diego, Y., & Lobo, J. (2008). Genetic  
523 consequences of habitat fragmentation in plant populations: susceptible signals in  
524 plant traits and methodological approaches. *Molecular Ecology*, *17*, 5177-5188. doi:  
525 10.1111/j.1365-294X.2008.03971.x

526 Aguilar, R., Calviño, A., Ashworth, L., Aguirre-Acosta, N., Carbone, L. M., Albrieu-  
527 Llinás, G., ... Cagnolo, L. (2018). Unprecedented plant species loss after a decade in  
528 fragmented subtropical Chaco Serrano forests. *Plos One*, *13*, e0206738. doi:  
529 10.1371/journal.pone.0206738

530 Aguilar, R., Cristóbal-Pérez, E. J., Balvino-Olvera, F. J., de Jesús Aguilar-Aguilar, M.,  
531 Aguirre-Acosta, N., Ashworth, L., ... & Quesada, M. (2019). Habitat fragmentation  
532 reduces plant progeny quality: a global synthesis. *Ecology letters*, *22*(7), 1163-1173.  
533 doi: 10.1111/ele.13272

534 Aldrich, P. R., Hamrick, J. L., Chavarriaga, P., & Kochert, G. (1998). Microsatellite  
535 analysis of demographic genetic structure in fragmented populations of the tropical  
536 tree *Symphonia globulifera*. *Molecular Ecology*, 7, 933-944. doi: 10.1046/j.1365-  
537 294x.1998.00396.x

538 Ally, D., & Ritland, K. (2006). A case study: looking at the effects of fragmentation on  
539 genetic structure in different life history stages of old-growth mountain hemlock  
540 (*Tsuga mertensiana*). *Journal of Heredity*, 98, 73-78. doi: 10.1093/jhered/esl048

541 Aparicio, A., Hampe, A., Fernández-Carrillo, L., & Albaladejo, R. G. (2012).  
542 Fragmentation and comparative genetic structure of four mediterranean woody  
543 species: complex interactions between life history traits and the landscape context.  
544 *Diversity and Distribution*, 18, 226-235. doi: 10.1111/j.1472-4642.2011.00823.x

545 Bakker, J., van Rijswijk, M. E. C., Weissing, F. J., & Bijlsma, R. (2010). Consequences  
546 of fragmentation for the ability to adapt to novel environments in experimental  
547 *Drosophila* metapopulations. *Conservation Genetics*, 11, 435-448. doi:  
548 10.1007/s10592-010-0052-5

549 Borcard, D., Gillet, F., & Legendre, P. (2011). *Numerical Ecology with R*. New York:  
550 Springer.

551 Bolger, A. M., Lohse, M., & Usadel, B. (2014). Trimmomatic: a flexible trimmer for  
552 Illumina sequence data. *Bioinformatics*, 30, 2114-2120. doi:  
553 10.1093/bioinformatics/btu170

554 Caswell, H. (2001). *Matrix Population Models: Construction, Analysis, and*  
555 *Interpretation*, 2nd edn. Sunderland: Sinauer Associates. Inc.

556 Coltman, D. W., Pilkington, J. G., Smith, J. A., & Pemberton, J. M. (1999). Parasite-  
557 mediated selection against inbred Soay sheep in a free-living island populaton.

558 *Evolution*, 53, 1259-1267. doi: 10.1111/j.1558-5646.1999.tb04538.x

559 Crow, J. F., & Morton, N. E. (1955). Measurement of gene frequency drift in small  
560 populations. *Evolution*, 9, 202-214. doi: 10.2307/2405589

561 Ellner, S. (1996). Environmental fluctuations and the maintenance of genetic diversity  
562 in age or stage-structured populations. *Bulletin of Mathematical Biology*, 58, 103-  
563 127. doi: 10.1016/0092-8240(95)00309-6

564 Ellner, S., & Hairston, N. G. Jr. (1994). Role of overlapping generations in maintaining  
565 genetic variation in a fluctuating environment. *American Naturalist*, 143, 403-417.  
566 doi: 10.1086/285610

567 González, A. V., Gómez-Silva, V., Ramírez, M. J., & Fontúrbel, F. E. (2020). Meta-  
568 analysis of the differential effects of habitat fragmentation and degradation on plant  
569 genetic diversity. *Conservation Biology*, 34(5), 711-720. doi: 10.1111/cobi.13422

570 Goudet, J. (2005). HIERFSTAT, a package for R to compute and test hierarchical F-  
571 statistics. *Molecular Ecology Note*. 5, 184-186. doi: 10.1111/j.1471-  
572 8278 .2004.00828.x

573 Hokkaido Government. (1897). *Hokkaido Shokuminchi Sentei Daini Houbun*. Sapporo:  
574 Hokkaido Government.

575 Hui, T. Y. J., & Burt, A. (2015). Estimating effective population size from temporally  
576 spaced samples with a novel, efficient maximum likelihood algorithm. *Genetics*,  
577 200, 285-293. doi: 10.1534/genetics.115.174904

578 Jombart, T. (2008). adegenet: a R package for the multivariate analysis of genetic  
579 markers. *Bioinformatics*, 24, 1403-1405. doi: 10.1093/bioinformatics/btn129

580 Kramar, A. T., Ison, J. L., Ashley, M. V., & Howe, H. F. (2008). The paradox of forest  
581 fragmentation genetics. *Conservation Biology*, 22(4), 878-885. doi: 10.1111/j.1523-

582 1739.2008.00944.x

583 Krauss, J., Bommarco, R., Guardiola, M., Heikkinen, R. K., Helm, A., Kuussaari, M., ...  
584 Steffan-Dewenter, I. (2010). Habitat fragmentation causes immediate and time-  
585 delayed biodiversity loss at different trophic levels. *Ecology Letters*, *13*, 597-605.  
586 doi: 10.1111/j.1461-0248.2010.01457.x

587 Lande, R. (1988). Genetics and demography in biological conservation. *Science*, *241*,  
588 1455-1460. doi: 10.1126/science.3420403

589 Leimu, R., Mutikainen, P., Koricheva, J., & Fischer, M. (2006). How general are  
590 positive relationships between plant population size, fitness and genetic variation?  
591 *Journal of Ecology*, *94*, 942-952. doi: 10.1111/j.1365-2745.2006.01150.x

592 Li, X. Y., Kurokawa, S., Giaimo, S., & Traulsen, A. (2016). How life history can sway  
593 the fixation probability of mutants. *Genetics*, *203*, 1297-1313. doi:  
594 10.1534/genetics.116.188409

595 Lowe, A. J., Boshier, D., Ward, M., Bacles, C. F. E., & Navarro, C. (2005). Genetic  
596 resource impacts of habitat loss and degradation; reconciling empirical evidence and  
597 predicted theory for neotropical trees. *Heredity*, *95*, 255-273. doi:  
598 10.1038/sj.hdy.6800725

599 Martins, E. M., Lamont, R. W., Martinelli, G., Lira-Medeiros, C. F., Quinet, A., &  
600 Shapcott, A. (2015). Genetic diversity and population genetic structure in three  
601 threatened *Ocotea* species (Lauraceae) from Brazil's Atlantic Rainforest and  
602 implications for their conservation. *Conservation Genetics*, *16*, 1-14. doi:  
603 10.1007/s10592-014-0635-7

604 Murray, M. G., & Thompson, W. F. (1980). Rapid isolation of high molecular weight  
605 plant DNA. *Nucleic Acids Research*, *8*, 4321-4326. doi: 10.1093/nar/8.19.4321

606 Nei, M., & Chesser, R. K. (1983). Estimation of fixation indices and gene diversities.  
607 *Annals of Human Genetics*, 47, 253-259. doi: 10.1111/j.1469-1809.1983.tb00993.x

608 Ohara, M., & Higashi, S. (1987). Interference by ground beetles with the dispersal by  
609 ants of seeds of *Trillium* species (Liliaceae). *Journal of Ecology*, 75, 1091-1098.  
610 doi: 10.2307/2260316

611 Ohara, M., & Kawano, S. (2005). Life-history monographs of Japanese plants. 2:  
612 *Trillium camschatcense* Ker-Gawl.(Trilliaceae). *Plant Species Biology*, 20, 75-82.  
613 doi: 10.1111/j.1442-1984.2005.00126.x

614 Ohara, M., Takeda, H., Ohno, Y., & Shimamoto, Y. (1996). Variations in the breeding  
615 system and the population genetic structure of *Trillium kamtschaticum* (Liliaceae).  
616 *Heredity*, 76, 476-484. doi: 10.1038/hdy.1996.70

617 Ohara, M., Tomimatsu, H., Takada, T., & Kawano, S. (2006). Importance of life history  
618 studies for conservation of fragmented populations: a case study of the understory  
619 herb, *Trillium camschatcense*. *Plant Species Biology*, 21, 1-12. doi: 10.1111/j.1442-  
620 1984.2006.00145.x

621 Oksanen, J., Blanchet, F. G., Friendly, M., Kindt, R., Legendre, P., McGlenn, D., ...  
622 Wagner, H. (2019). vegan: community ecology package. R package version 2.5-3.  
623 Retrieved from <https://CRAN.R-project.org/package=vegan>

624 Ramsayer, J., Kaltz, O., & Hochberg, M. E. (2012). Evolutionary rescue in populations  
625 of *Pseudomonas fluorescens* across an antibiotic gradient. *Evolutionary*  
626 *Applications*, 6, 608-616. doi: 10.1111/eva.12046

627 Reed, D. H., & Frankham, R. (2003). Correlation between fitness and genetic diversity.  
628 *Conservation Biology*, 17(1), 230-237. doi: 10.1046/j.1523-1739.2003.01236.x

629 Rochette, N. C., Rivera-Colón, A. G., & Catchen, J. M. (2019). Stacks 2: Analytical

630 methods for paired-end sequencing improve RADseq-based population genomics.  
631 *Molecular Ecology*, 28, 4737-4754. doi: 10.1111/mec.15253

632 Silvertown, J., Franco, M., Pisanty, I., & Mandoza, A. (1993). Comparative plant  
633 demography – relative importance of life-cycle components to the finite rate of  
634 increase in woody and herbaceous perennials. *Journal of Ecology*, 81, 465-476. doi:  
635 10.2307/2261525

636 Stoffel, M. A., Esser, M., Kardos, M., Humble, E., Nichols, H., David, P., & Hoffman, J.  
637 I. (2016). inbreedR: an R package for the analysis of inbreeding based on genetic  
638 markers. *Methods in Ecology and Evolution*, 7, 1331-1339. doi: 10.1111/2041-  
639 210X.12588

640 Suyama, Y., & Matsuki, Y. (2015). MIG-seq: an effective PCR-based method for  
641 genome-wide single-nucleotide polymorphism genotyping using the next-generation  
642 sequencing platform. *Scientific Reports*, 5, 16963. doi: 10.1038/srep16963

643 Takada, T., & Kawai, Y. (2020). An analysis of elasticity vector distribution specific to  
644 semelparous species using randomly generated population projection matrices and  
645 the COMPADRE Plant Matrix Database. *Ecological Modelling*, 431, 109125. doi:  
646 10.1016/j.ecolmodel.2020.109125

647 Toczydlowski, R. H., & Waller, D. M. (2019). Drift happens: Molecular genetic  
648 diversity and differentiation among populations of jewelweed (*Impatiens capensis*  
649 Meerb.) reflect fragmentation of floodplain forests. *Molecular Ecology*, 28, 2459-  
650 2475. doi: 10.1111/mec.15072

651 Tomimatsu, H., & Ohara, M. (2002). Effects of forest fragmentation on seed production  
652 of the understory herb *Trillium camschatcense*. *Conservation Biology*, 16, 1277-  
653 1285. doi: 10.1046/j.1523-1739.2002.00412.x

654 Tomimatsu, H., & Ohara, M. (2003). Genetic diversity and local population structure of  
655 fragmented populations of *Trillium camschatcense* (Trilliaceae). *Biological*  
656 *Conservation*, *109*, 249-258. doi: 10.1016/S0006-3207(02)00153-2

657 Tomimatsu, H., & Ohara, M. (2004). Edge effects on recruitment of *Trillium*  
658 *camschatcense* in small forest fragments. *Biological Conservation*, *117*, 509-519.  
659 doi: 10.1016/j.biocon.2003.08.010

660 Tomimatsu, H., & Ohara, M. (2006). Evaluating the consequences of habitat  
661 fragmentation: a case study in the common forest herb *Trillium camschatcense*.  
662 *Population Ecology*, *48*, 189-198. doi: 10.1007/s10144-006-0269-9

663 Tomimatsu, H., & Ohara, M. (2010). Demographic response of plant populations to  
664 habitat fragmentation and temporal environmental variability. *Oecologia*, *162*, 903-  
665 911. doi: 10.1007/s00442-009-1505-8

666 Waples, R. S., & Teel, D. J. (1990). Conservation genetics of Pacific salmon I. temporal  
667 changes in allele frequency. *Conservation Biology*, *4*, 144-156. doi: 10.1111/j.1523-  
668 1739.1990.tb00103.x

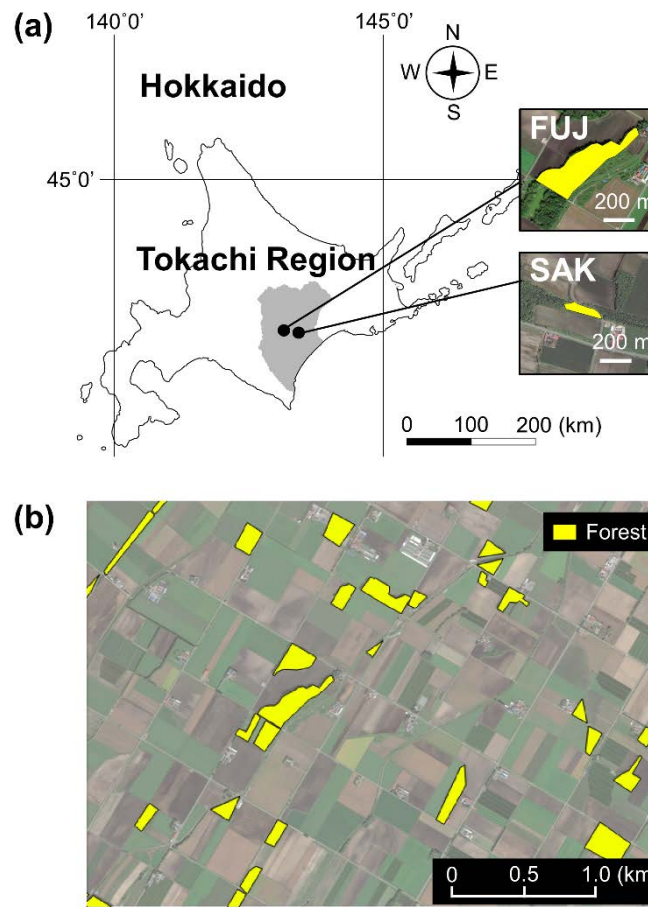
669 Williams, S. L. (2001). Reduced genetic diversity in eelgrass transplantations affects  
670 both population growth and individual fitness. *Ecological Applications*, *11*(5), 1472-  
671 1488. doi: 10.1890/1051-0761(2001)011[1472:RGDIET]2.0.CO;2

672 Young, A., Boyle, T., & Brown, T. (1996). The population genetic consequences of  
673 habitat fragmentation for plants. *Trends in Ecology and Evolution*, *11*, 413-418. doi:  
674 10.1016/0169-5347(96)10045-8

675

676

677

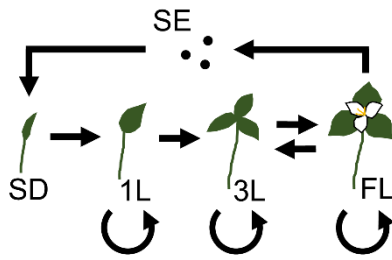


678

679 **Figure 1.** (a) The location of the Tokachi region and the two studied populations: SAK  
 680 (Sakuragi, small population) and FUJ (Fuji, large population). (b) An iconic aerial view  
 681 of fragmented forests in the Tokachi region

682





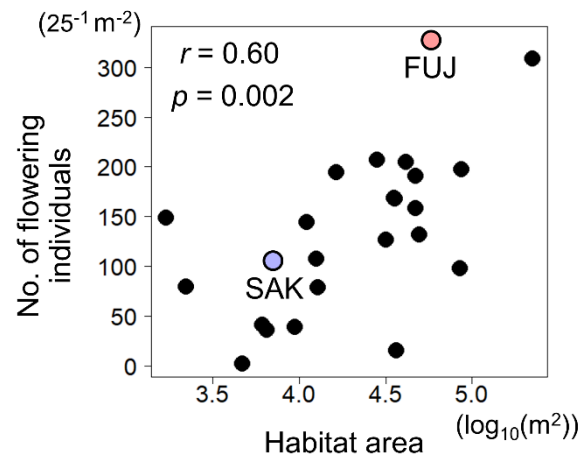
683

684 **Figure 2.** Life history of *Trillium camschatcense*. Arrows represent the possible annual

685 trajectory of individuals. SE, seed; SD, seedling; 1L, one-leaf; 3L, three-leaves; FL,

686 flowering

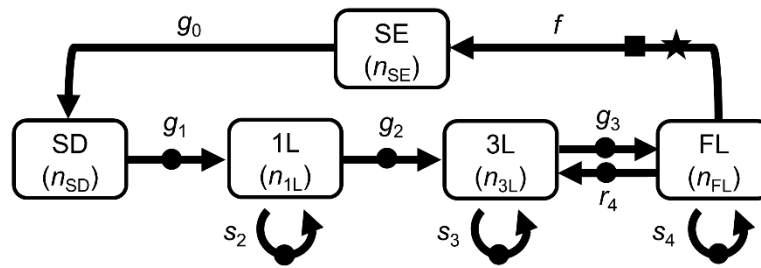
687



688

689 **Figure 3.** A positive effect of habitat area on the density of flowering individuals  
 690 revealed by preliminary survey in 2018. Blue and red circles represent the data of SAK  
 691 (Sakuragi) and FUJ (Fuji) population, respectively

692

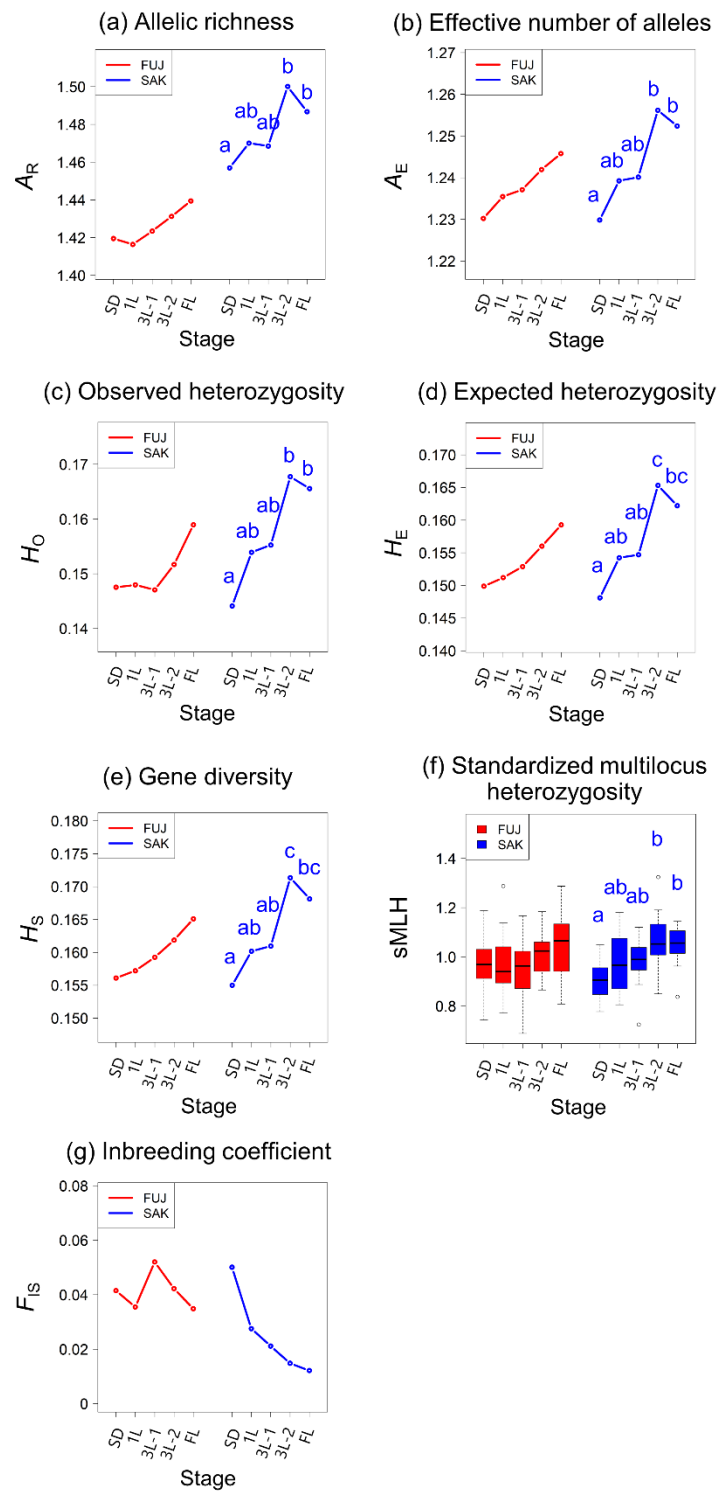


- ★ Genetic drift (multinomial sampling of  $N_b$  seeds)
- Demographic stochasticity (multinomial sampling)
- Demographic stochasticity (Poisson sampling)

693

694 **Figure 4.** Population updating rules used in simulation analyses.  $g_0$  is germination rate  
 695 of SE (seed).  $g_1$ ,  $g_2$ , and  $g_3$  are the growth rates of SD (seedling), 1L (one-leaf), and 3L  
 696 (three-leaves).  $s_2$ ,  $s_3$ , and  $s_4$  are the stasis rates of 1L, 3L, and FL (flowering).  $r_4$  and  $f$   
 697 are the retrogression rate and fecundity of FL. At each timestep (year), the fate of  
 698 individuals was determined depending on these demographic rates. When incorporating  
 699 genetic drift (scenario 2 and 4), we did multinomial sampling  $N_b$  times to determine the  
 700 genotype frequencies of SE (seed), as marked with star symbol. When incorporating  
 701 demographic stochasticity (scenario 3 and 4), we applied multinomial and Poisson  
 702 sampling at transitions marked with circle and square, respectively. The number of  
 703 individuals were kept constant (SE,  $n_{SE}$ ; SD,  $n_{SD}$ ; 1L,  $n_{1L}$ ; 3L,  $n_{3L}$ ; FL,  $n_{FL}$ ) by scaling  
 704 at each time step

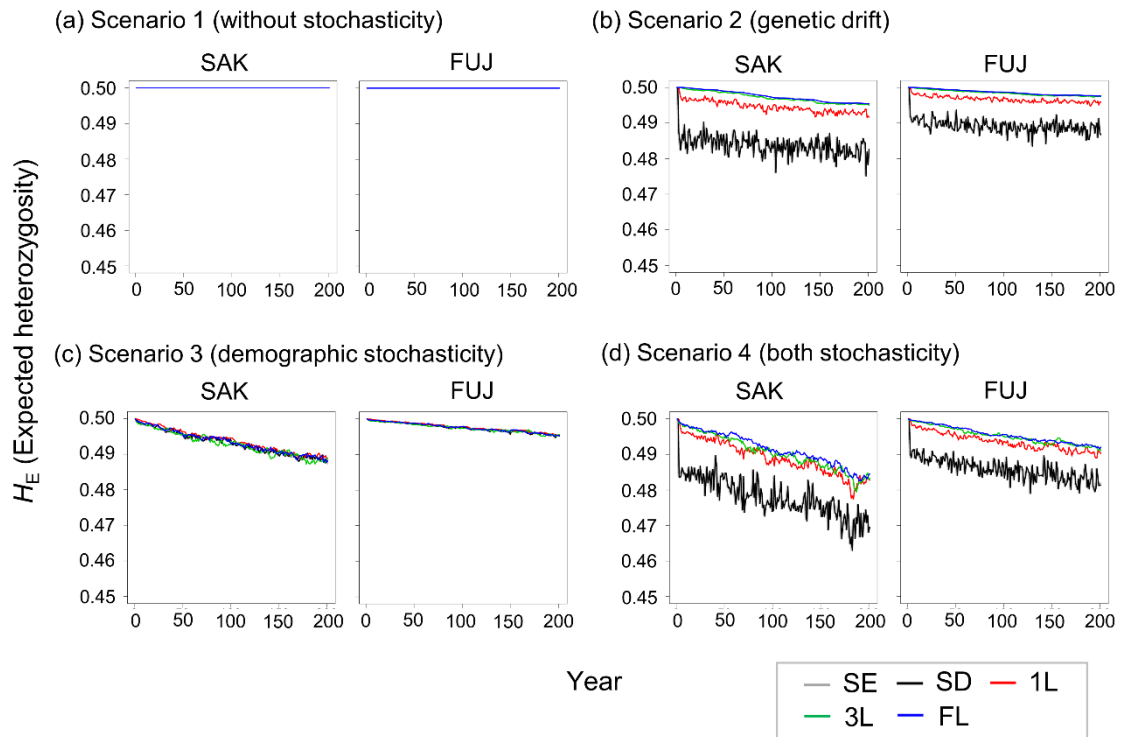
705



706

707 **Figure 5.** (a) Allelic richness  $A_R$ , (b) effective number of alleles  $A_E$ , (c) observed  
 708 heterozygosity  $H_O$ , (d) expected heterozygosity  $H_E$ , (e) gene diversity  $H_S$ , (f)  
 709 standardized multilocus heterozygosity sMLH, and (g) inbreeding coefficient  $F_{IS}$  at each

710 life history stage (SE (seed), SD (seedling), 1L (one-leaf), 3L (three-leaves), and FL  
711 (flowering)) of both populations. Data shown in red and blue are that of FUJ (Fuji, large  
712 population) and SAK (Sakuragi, small population), respectively. sMLH, which was  
713 estimated per individual, are shown in box plot, while the other indices estimated per  
714 stage are shown in dots. Significant difference was detected by permutation test for pairs  
715 marked with different alphabets (significance level = 0.05). No alphabet signs are  
716 assigned when there were no statistically significant differences  
717

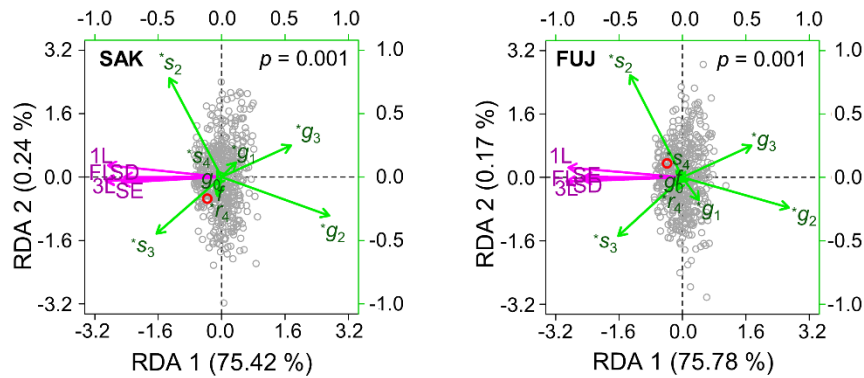


718

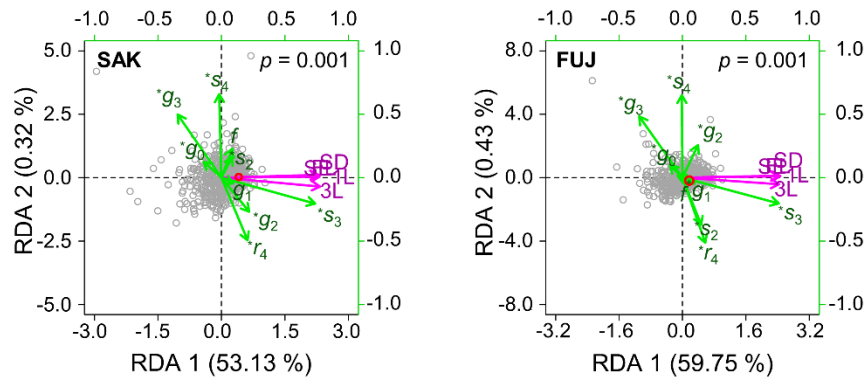
719 **Figure 6.** Temporal changes in expected heterozygosity ( $H_E$ ) of the five stages (SE (seed),  
 720 SD (seedling), 1L (one-leaf), 3L (three-leaves), and FL (flowering)) in SAK (Sakuragi,  
 721 small population) and FUJ (Fuji, large population) under the four scenarios: no  
 722 stochasticity (scenario 1), genetic drift (scenario 2), demographic stochasticity (scenario  
 723 3), and both genetic drift and demographic stochasticity (scenario 4)

724

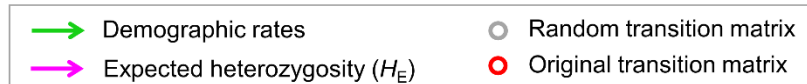
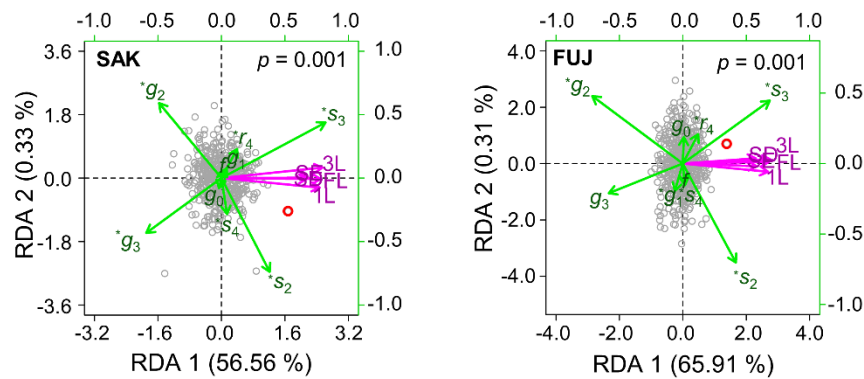
(a) Scenario 2 (genetic drift)



(b) Scenario 3 (demographic stochasticity)



(c) Scenario 4 (both stochasticity)



725

726 **Figure 7.** RDA correlation triplots of SAK (Sakuragi, small population) and FUJ (Fuji,  
 727 large population) under genetic drift (scenario 2), demographic stochasticity (scenario 3),  
 728 and both (scenario 4). Top and right-hand axes are for constraints (demographic rates),  
 729 while bottom and left-hand axes are for  $H_E$  of the five stages (SE (seed), SD (seedling),

730 1L (one-leaf), 3L (three-leaves), and FL (flowering)) and ordinated 501 trials. For each  
731 panel, the angles among arrows reflect their correlations: those in the same direction have  
732 positive correlations, while those in the opposite direction have negative correlations. *P*  
733 values of the overall ordination were shown at the topright margin of each figure. \*  
734 denotes constraint variables significantly constituting the ordination (significance level =  
735 0.05). Percentages presented in axis labels indicate the explanatory power of the axes